Extension of discrete tribocharging models to continuous size distributions

Dylan Carter and Christine Hartzell

Phys. Rev. E **95**, 012901 — Published 23 January 2017

DOI: 10.1103/PhysRevE.95.012901

An Extension of Discrete Tribocharging Models to Continuous Size Distributions

Dylan Carter and Christine Hartzell
University of Maryland
(Dated: October 24, 2016)

Triboelectric charging, the phenomenon by which electrical charge is exchanged during contact between two surfaces, has been known to cause significant charge separation in granular mixtures, even between chemically identical grains. This charging is a stochastic size-dependent process resulting from random collisions between grains. The prevailing models and experimental results suggest that, in most cases, larger grains in a mixture of dielectric grains acquire a positive charge, while smaller grains charge negatively. These models are typically restricted to mixtures of two discrete grain sizes, which are not representative of most naturally-occurring granular mixtures, and neglect the effect of grain size on individual charging events. We have developed a new model that predicts the average charge distribution in a granular mixture, for any continuous size distribution of dielectric grains of a single material. Expanding to continuous size distributions enables the prediction of charge separation in many natural granular phenomena, including terrestrial dust storms and industrial powder handling operations. The expanded model makes new predictions about the charge distribution, including specific conditions under which the usual size-dependent polarity is reversed such that larger grains charge negatively.

I. INTRODUCTION

Granular mixtures are susceptible to the generation of large electrical potential differences due to triboelectric charging, even when all grains are composed of the same material. This phenomenon is connected to the large electrical fields that often develop in sand storms [1–3] and ash clouds [4], and causes clumping and even dust explosions in powder-handling industries [5–8]. This type of charge exchange is stochastic due to the chemical symmetry among all grains, but trends can be observed in the charging behavior. Most experiments and existing models for charge exchange predict that larger grains will tend to acquire a positive charge and smaller grains will become negatively charged, on average. The degree of charge separation is influenced primarily by the size differences and mass fractions of each discrete grain size [9–13]. Existing models for charge exchange in granular mixtures of a single material neglect a number of important effects, especially the influence of contact area during collisions and the effect of non-discrete size distributions on charge separation, and typically underestimate the magnitude of the charge exchange [9, 10, 14].

In this paper, we expand existing models of tribocharging to make predictions about the charge distribution in mixtures with a continuous size distribution. To date, analytical models for charge exchange typically apply only to very simple mixtures of grains in which each grain is assumed spherical and has one of two allowed sizes [1, 9–12, 14]. Many of these models describe charge exchange events as identical for all pairs of grains regardless of grain size, despite the fact that the final charge is observed to be size-dependent [9–13]. Because the magnitude of insulator tribocharging is shown to be highly dependent on the area in contact [13, 15–18], we introduce an additional term A_{ij}, the contact area between grains of radii R_i and R_j during a collision. This causes the amount of transferred charge during a collision to depend upon the relative sizes of the grains in contact, changing the properties of the charge distribution and making new predictions about charging trends for various size distributions.

II. EXISTING MODELS FOR GRANULAR TRIBOCHARGING

Tribocharging occurs between nearly every combination of materials, including conductors, semiconductors, and insulators. There are many different mechanisms and models for the charge exchange depending on properties of the materials. For example, in conductive materials in contact, mobile electrons in the bulk are able to easily transfer to materials with lower surface energy, allowing predictable exchange of charge that disperses evenly throughout the materials [19].

Insulators, however, exhibit far more complex charging patterns, with charge exchange attributed to many causes with various degrees of success. For the contact of metals with insulators, an empirically-determined effective work function admits treatment

of the charge exchange in a similar fashion to the high-conductivity case [19, 20]. However, the contact of insulators with other insulators is far less well understood. While the degree and cause of charge transfer is difficult to identify in many such cases, the direction is fairly predictable, with a particular charge polarity frequently arising after contact between certain pairs of materials. For this reason, researchers have developed a triboelectric series that lists materials in order of polarity, used to predict the direction of charge transfer when two materials from the series come into contact [21, 22]. These lists are qualitative and often unreliable due to the wide variety of possible mechanisms causing insulator charging: charge exchange has been attributed to such factors as the settling of trapped high-energy electrons [9–12, 16, 17], the release of adsorbed ions [8], breaking of polymer chains [23], and interactions with atmospheric ions [15], with varying degrees of accuracy.

It has also been shown that tribocharging occurs even between identical materials, despite the lack of chemical differences between the surfaces. Based on their experiments, Lowell and Truscott proposed a model in which a number of electrons on insulator surfaces are in unfavorably high-energy states, but cannot reach low energy states due to the low conductivity of the material. During contact with another surface, these electrons are exposed to low-energy states on the other surface and can be transferred [16, 17]. Shinbrot, Komatsu, and Zhao demonstrated that rubbing two identical insulating surfaces together in air produces an increasingly large potential difference, with the surfaces acquiring a random polarity in each experiment [15]. In general, the symmetry of same-material tribocharging causes the direction and magnitude of charge exchange to vary between experiments, suggesting that a stochastic model (e.g., high-energy electron transfer) will be more successful than previous rigidly deterministic models (e.g., the work function difference).

Granular mixtures of a single insulating material are just as susceptible to same-material tribocharging as flat surfaces. In many cases, granular mixtures include a variety of materials, and their charge distribution is governed by these material differences; for example, pneumatic powder transport often induces significant triboelectric exchange between powders and metal surfaces [5–8]. In addition, humidity in the air and adsorbed onto grain surfaces has been shown to significantly alter charging characteristics [8, 24]. However, even granular mixtures of only a single insulating material have been shown to readily develop charge separation through same-material particle-particle collisions [10, 12, 25].

Expanding upon Lowell and Truscott's model for trapped electron relaxation in insulator-insulator contact, Lacks and Levandovsky proposed a mechanism for grain charging due to size differences in a mixture alone [9]. During agitation of a granular mixture, grains repeatedly collide and slide against each other, allowing all trapped electrons to achieve lower-energy states. Lacks and Levandovsky developed a model for predicting the average steady-state charge on grains of a particular size in a bidisperse mixture of a single material, demonstrating that larger grains will always acquire a positive charge in such a case. They later expanded upon this model to include the more general case of multiple size species and the possibility for low-energy electron exchange, although they neglected the latter in simulations and analysis [11].

Particle dynamics simulations of this "population balance" model compare favorably with experimental results, with larger grains acquiring a more positive charge on average than smaller grains [9, 11, 13]. Forward, Lacks, and Sankaran developed a methodology for isolating particle-particle interactions through the use of a bed fluidized with inert nitrogen [26]. In a variety of experiments, they demonstrated that the size-dependent charge polarity predicted by the electron relaxation model is independent of material and occurs in any mixture with a wide size distribution [12, 27, 28]. They further showed that the degree of charge separation is highly dependent on the relative masses of each size species, as this value influences the rate at which grains collide with other species. In 2009, Lacks and Kok extended the model to include a dependence of the quantity of transferred charge on the sizes of the grains in contact [14]. In their model, electrons transfer due to tunneling during collisions, with the probability of tunneling a function of the distance between the electron on one grain and the closest point on the surface of the other grain. Assuming δ_0 is the maximum distance an electron in the ground state could tunnel, one can calculate the surface area on each grain over which electrons are able to transfer.

Jaeger and Waitukaitis, *et al*, developed a more sophisticated method for measuring the actual charge on each grain to further investigate the predictions of these models [10, 29]. Their results also agreed with the polarity predicted by the original model, but they observed that the magnitude of the charge was too large to be simply caused by trapped electrons. They suggested that alternative mechanisms

such as ion transfer or interactions with the atmosphere may play a role in charging.

Although the experimental evidence for Lacks and Levandovsky's model is promising, the model itself is strikingly simplistic. In their initial discussion, Lacks and Levandovsky note that they have ignored a variety of phenomena, including the effect of aspherical shapes, sliding contact, and electrostatic forces between grains, which may alter the charge exchange rate [9]; Kok and Lacks similarly leave out these factors [14]. We have modified these models by including a new method for calculating contact area differences between grains, which drive the amount of charge exchanged during a collision. When two real objects collide, they deform slightly such that they develop an approximately flat contact area between them, across which trapped electrons are able to move. By assuming each collision exchanges a size-independent number of electrons from each grain, Lacks and Levandovsky neglect the effect of grain size differences and assume electron transfer rate is independent of collision area. This area is determined by the size and collision energy of the grains, and therefore increases with increasing grain size. Experiments on sphere-to-surface contact charging have demonstrated that the exchanged charge is indeed proportional to contact area, and that contact area can be varied through changes in collision speed and sphere size [18, 30, 31]. While the contact area formulation in Kok and Lacks' work also suggests a proportional relationship between collision area and transferred charge, it requires that grains are treated as hard spheres, so that changes in collision energy have no effect on the charge [14].

In the model we develop below, we include the effects of grain size on the number of electrons transferred per collision and extend Lacks and Levandovsky's model from a finite number of discrete grain sizes to a continuous distribution function. As with the population balance model, we assume that all grains of approximately the same size can be represented by a single average grain, and we track its behavior over time to estimate the accumulated charge. We will also attempt to determine whether or not this model more accurately represents real granular mixtures than other related models, why it differs from experimental observations, and the implications for our understanding of granular tribocharging as a whole. The results of this model will be explored in future experiments to examine the accuracy of the inclusion of the collision area term and the conditions under which it has an effect on the charging.

III. GRAIN CHARGING MODEL

For the purposes of this model, we will adopt the charge transfer mechanism proposed by Lowell and Truscott [16, 17] and further elaborated by Lacks and Levandovsky [9, 11]. Each grain is assumed to be a solid sphere of radius R; its surface area is therefore $4\pi R^2$. The surface area density of trapped high-energy electrons is ρ_H and is initially the same for all grains. Its value at time $t = 0$ (before charge exchange due to mixing) is given by ρ_0, at which time all grains are electrically neutral. According to the trapped electron model, each collision exposes some number of high-energy electrons that each have a random probability of being transferred; we will denote this probability as f_H. In addition, we will assume that each collision involves some characteristic contact area A_{ij}, where the colliding grains have radii R_i and R_j. We will further assume that the relative speed between grains is size-independent and equal for all grains, and they are all composed of the same material; therefore, the contact area is a function of the grains' radii only. This allows us to express the number of high-energy electrons transferred from a grain of radius R_i to a grain of radius R_j as $f_H \rho_{H,i} A_{ij}$. Note that the average surface density of electrons $\rho_{H,i}$ is a function of time, and therefore varies throughout the mixing process.

A. Collisions

In order to estimate the collision rates between grains, we assume that all grains move at approximately the same speed, and therefore that the average relative speed between two grains is a constant, here called v_r. For very small particles, the kinetic energy is frequently governed by thermal effects and the electromagnetic force, resulting in size- and/or charge- dependencies for the particle speed. However, we will assume for this model that the motion of the grains is dominated by some other external force that gives each grain an average speed of v_r relative to the other grains in the bulk, e.g. a uniform acceleration applied to a bed of loose grains. See Figure 1 for an illustration of this collision process.

We can use the relative speed between grains to estimate the collision rates as grains move through the mixure. Consider a single grain of radius R_i moving against a background of grains of radius R_j. The first grain moves with speed v_r relative to the background grains. In some time Δt, the

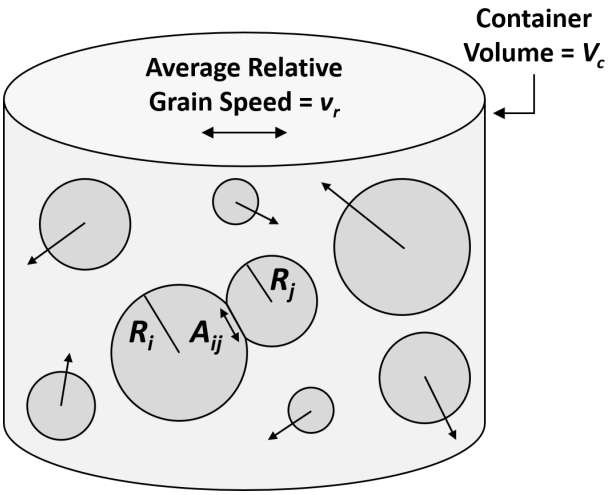

FIG. 1: Diagram of physical system considered. Grains with a normalized size distribution given by $g(R)$ are mixed in a container of volume V_c. Mixing is performed by moving the container with average speed v_r, such that the grains inside also move with average speed v_r. The grains are then assumed to move in random directions with average speed v_r as well. When a grain of radius R_i collides with a grain of radius R_j, some contact area is formed in region A_{ij}. High-energy electrons in this region are capable of transferring between the two grains and settling into stable low-energy states.

grain moves a distance $v_r \Delta t$. In this time, it collides with any grains whose centers are a distance $R_i + R_j$ from the axis of its motion. Therefore, the moving grain collides with any grains within the volume $\pi \left(R_i + R_j\right)^2 v_r \Delta t$. If our control volume is V_c and there are n_j grains with radius R_j in the mixture, then the rate at which our grain of radius R_i collides with grains of radius R_j is ω_{ij}, where:

$$\omega_{ij} = \frac{\pi v_r n_j}{V_c} \left(R_i + R_j\right)^2 \tag{1}$$

B. Size Distribution

Previous tribocharging models have been developed specifically for application to size distributions consisting of two discrete sizes [9, 12]. These models are restrictive, as unsieved granular mixtures in nature are more accurately represented by continuous size distribution functions. While bidisperse mixtures are much easier to manipulate analytically and are relevant to simple tribocharging experiments, they cannot explain or predict phenomena in natural granular mixtures. Thus, we will consider charge exchange in an arbitrary continuous grain size distribution.

Consider a mixture of grains with a probability distribution of radii given by $g(R)$. That is, the fraction of grains in the mixture with a radius within dR of R is $g(R)$. The distribution is normalized such that $\int_0^\infty g(R) dR = 1$. As a result, the number of grains with radius R_j (defined as n_j) is equal to $n_0 g(R) dR$, where n_0 is the total number of grains in the mixture. To find the value of n_0, we define the total mass of the mixture as M_0; we use this parameter because of the ease with which this is directly measured in experiments. Using this definition, and defining the mass density of grains as ρ_M, we can determine n_0 by integrating the mass of all grains in the mixture as follows:

$$M_0 = \frac{4}{3} \pi \rho_M n_0 \int_0^\infty R^3 g(R) dR \tag{2}$$

The use of a continuous size distribution also has important implications for the collision rate. Recall that the collision rate ω_{ij} depends upon the number of grains n_j of radius R_j in the mixture. When we expand this term, we get a differential term dR_j in the definition of ω_{ij}. This will be important when we calculate the rate at which high-energy electrons are transferred to the mixture background.

C. Electron Transfer Rates

We begin by considering the rate at which a single grain of radius R_i loses electrons to low-energy states on grains of radius R_j during mixing. We have previously derived an expression for the frequency of such collisions ω_{ij}, as well as an expression for the number of electrons transferred per collision at a given time t. Suppose that the charge and number of acquired electrons on a grain does not affect the rate at which it continues to donate or acquire electrons during collisions. We can then write an expression for the rate at which high-energy electrons on a grain of radius R_i are lost:

$$\frac{d}{dt} \left(\rho_{H,i}\right) |_{R_j} = -\frac{\omega_{ij} f_H \rho_{H,i} A_{ij}}{4 \pi R_i^2} \tag{3}$$

This expression gives only the rate at which electrons are lost to grains in a narrow band of radii

around R_j. To obtain the rate at which the grain loses electrons to all other grains in the mixture background, we integrate this expression over the range of all grain sizes R_j:

$$\frac{d\rho_{H,i}}{dt} = -\alpha_i \rho_{H,i} \tag{4}$$

$$\alpha_i = \frac{v_r n_0 f_H}{4R_i^2 V_c} \int_0^\infty A_{ij} \left(R_i + R_j\right)^2 g(R_j) dR_j \tag{5}$$

For the time being, since we have not defined an expression for A_{ij}, we cannot evaluate this integral. We shall find that for most size distributions, it will be necessary to evaluate this integral numerically.

1. Electron Loss Fraction

In the previous section, we defined the average rate at which a single grain of radius R_i, representating the average grain of that radius, loses high-energy electrons to grains of radius R_j. As we saw, this rate is given as a continuous function (averaged over the discrete collision events that happen over much smaller time scales) and is directly proportional to the electron density $\rho_{H,i}(t)$. Suppose that we wished to find the fraction of all electrons currently being transferred from a grain of radius R_i that were going to grains of a specific size R_j. This quantity is critical to understanding the nature of size-dependent charge separation. We note that this quantity, here called f_{ij}, can be equivalently described as the ratio between the rate of electron transfer to size species R_j, given by Equation (3), and the rate of overall electron transfer to grains of all sizes, given by Equation (4):

$$f_{ij} = \frac{A_{ij} \left(R_i + R_j\right)^2 g(R_j) dR_j}{\int_0^\infty A_{ik} \left(R_i + R_k\right)^2 g(R_k) dR_k} \tag{6}$$

We have replaced the variable of integration R_j in the denominator with the dummy variable R_k, to distinguish it from the actual variable R_j in the numerator, the size of the grain band with which our single grain is colliding. Note that the electron density cancels out, and the fraction of electrons transferred is a constant fraction with a dependence on grain radii and the size distribution only. Importantly, we note that we can now express the rate of change of the high-energy electron population in the following simple ways:

$$\frac{d\rho_{H,i}}{dt}|_{R_j} = f_{ij} \frac{d\rho_{H,i}}{dt} = -\alpha_i f_{ij} \rho_{H,i} \tag{7}$$

2. Collision Area

Now that we have identified all the required relationships to make predictions about the average final charge, we turn our attention to the collision area. For the analysis up to this point, we have assumed that each grain is a hard sphere of a particular radius R. The contact area between two perfectly spherical hard grains is simply a point, but such a model neither contributes to our understanding of granular tribocharging nor fits experimental data regarding tribocharging in general. In experiments on rubbing flat surfaces together, the exchanged charge is directly proportional to the area exposed to contact, and collisions between small grains slide against each other rather than simply rebound at a point contact [18, 30, 31]. From this observation, we may conclude that the exchange of charge in real collisions between grains will be heavily dependent on the size of the grains. Specifically, because electron transfer in other systems tends to depend on the surface area, we expect to see a similar area dependence in sliding grain collisions.

The inclusion of a collision area term is a stark departure from the typical approach used in many granular tribocharging models. The model developed by Lacks and Levandovsky, and frequently employed to make predictions in various tribocharging experiments, assumes that a constant number of electrons (frequently one) is transferred during each collision. This is analogous to the assertion that $1 = f_H A_{ij} \rho_{H,i}(t)$, using the framework developed for our model. While this appears to create problems due to the fact that $\rho_{H,i}$ loses its dependence on time, we note that in the loss fraction f_{ij} (which we will later see is the most important term in predicting the final charge), the electron density divides out. Therefore, in calculating the final charge on the grains, the result is identical to the assumption that A_{ij} is a constant and also divides out. Other models have also been developed to include a contact area term, especially that of Kok and Lacks [14]; however, we believe that our implementation better represents what is known about the relationship between collision speed and transferred charge. In using a "maximum tunneling distance" as the effective boundary of the contact area, Kok and Lacks have developed a framework in which the effective contact

area is different for the two grains, due to the difference in surface curvature [14]. In our model, the contact area is the same for the two grains, which agrees with previous experiments and models exploring the effect of collision energy on contact area and transferred charge [15–18].

In Gugan's treatment of Hertz's theory [32], the collision area is given in terms of the collision speed U, reduced radius $R_* = \frac{R_i R_j}{R_i + R_j}$, reduced mass $M_* = \frac{m_i m_j}{m_i + m_j} = \frac{4\pi\rho_M R_i^3 R_j^3}{3\left(R_i^3 + R_j^3\right)}$, and effective elastic coefficient $X_* = \frac{1-\nu_i^2}{E_i} + \frac{1-\nu_j^2}{E_j} = \text{constant}$. Because we are here assuming that all grains are of the same material, they all have the same density, modulus E, and Poisson's ratio ν. We have also assumed that the relative speed between any two grains is v_r, so all factors involving only these terms can be dropped for simplicity:

$$A_{ij}^{2.5} = 16.4 v_r^2 M_* R_*^2 X_* \propto M_* R_*^2 \tag{8}$$

Now we expand these quantities and solve for A_{ij}:

$$A_{ij} \propto r_{ij} R_i R_j \tag{9}$$

$$r_{ij} = \frac{2^{1.2} R_i R_j}{\left(R_i^3 + R_j^3\right)^{0.4} \left(R_i + R_j\right)^{0.8}} \tag{10}$$

Because we are considering an area term, we have rearranged the expression so that it can be written as the product of the radii of the involved grains and a non-dimensional term r_{ij}. Note that this looks very similar to the square of the reduced radius defined above. This makes logical sense, as real collisions are not simply point contacts and will involve an amount of contact area highly dependent on the size and shape of the grains.

IV. STEADY-STATE GRAIN CHARGE SOLUTIONS

A. Solutions for Continuous Size Distributions

To predict the grain charge at some time t after the initiation of mixing, we must first calculate the rate at which a single grain accumulates low-energy electrons. Consider now that each grain of radius R_j gives a fraction f_{ji} of its high-energy electrons to grains of radius R_i. The rate at which electrons are given in this way after some time t is $-4\pi R_j^2 n_j f_{ji} \frac{d\rho_{H,j}}{dt}$. Therefore, if we divide this quantity by n_i, the number of grains of radius R_i, we get the rate of low-energy electron settling on the average grain of size R_i. Using Equation (4), the change in charge $Q_{L,ij}(t)$ contributed by these low-energy electrons from grains of radius R_j is:

$$\frac{dQ_{L,ij}}{dt} = -4e\pi\alpha_j R_j^2 f_{ji} \frac{n_j}{n_i} \rho_{H,j} \tag{11}$$

To obtain the overall contribution to the charge from all other grain sizes, we simply integrate this expression over all sizes R_j. Meanwhile, the grain is also losing high-energy electrons due to each of these collisions. The rate at which it loses electrons can be given as the rate of change of surface electron density (found above) multiplied by the surface area and electron charge $-e$:

$$\frac{dQ_{H,i}}{dt} = -4e\pi R_i^2 \frac{d\rho_{H,i}}{dt} = 4e\pi\alpha_i R_i^2 \rho_{H,i} \tag{12}$$

The overall rate of change of the charge of a single grain of radius R_i will be given by the sum of these rates:

$$\frac{dQ_i}{dt} = \frac{dQ_{H,i}}{dt} + \int_{dR_j} \frac{dQ_{L,ij}}{dt} \tag{13}$$

Recall from Equation (4) that the surface electron density can be written as an exponential decay function, with $\rho_{H,i}(t) = \rho_0 e^{-\alpha_i t}$. We can make this substitution and integrate over time to obtain an expression for the actual charge at time t:

$$\begin{aligned} Q_i(t) = 4e\pi\rho_0 \Bigg[& R_i^2 \left(1 - e^{-\alpha_i t}\right) \\ & - \int_0^\infty R_j^2 f_{ji} \frac{n_j}{n_i} \left(1 - e^{-\alpha_j t}\right) \Bigg] \end{aligned} \tag{14}$$

The above expression accounts for the fact that, at time $t = 0$, the grains are electrically neutral. By taking the time to infinity, we get an expression for the charge once all high-energy electrons have settled into low-energy states. This causes the exponential terms to die out, leaving only the following expression:

$$Q_{i,final} = 4e\pi\rho_0 \Bigg(R_i^2 - \int_0^\infty \frac{R_j^2 A_{ij} \left(R_i + R_j\right)^2 g(R_j) dR_j}{\int_0^\infty A_{jk} \left(R_j + R_k\right)^2 g(R_k) dR_k} \Bigg) \quad (15)$$

Equation (15) is an expression for the final charge on a grain of arbitrary size R_i in a mixture of grains with size distribution $g(R)$ after all mobile charges have settled into their preferred states. From the definition of the contact area, we can see that these integrals do not have an obvious closed-form solution (although the complexity is significantly reduced by applying Lacks and Levandovsky's equal contact area assumption). In addition, the use of an arbitrary size distribution function also prevents us from directly solving the integral in the general case. Therefore, solutions to the final charge equation must be obtained through numerical integration. This will be especially useful in the case of unusual size distribution functions, such as Taylor series curve fits to granular mixtures found in nature, where analytical solutions introduce unnecessary complexity.

B. Solutions for Discrete Size Distributions

Although a continuous size distribution is a better approximation of a real granular mixture than a set of discrete sizes, it is still instructive to explore how this model behaves in the case of a discrete size distribution, in order to allow comparison to both Lacks and Levandovsky's original model and to experimental observations. As discussed previously, most existing models to predict charging in laboratory mixtures employ a discrete size distribution, typically of only two primary grain radii, which we will here call R_1 and R_2, where R_1 is the larger size. This size distribution can be represented by a sum of two Dirac delta functions, which can be thought of as infinitely narrow normal distributions such that only two grain sizes are represented. Therefore, our size distribution will look like:

$$g(R) = \frac{k_1\delta_1 + k_2\delta_2}{k_1 + k_2}, \qquad \delta_i = \delta\left(R - R_i\right) \quad (16)$$

The weights k_1 and k_2 are related to the mass of each size species. The mass of a single species i is given by the following expression:

$$M_i = \frac{4\pi\rho_M n_0 k_i R_i^3}{3\left(k_1 + k_2\right)} \quad (17)$$

We can define a set of non-dimensional constants $d = \frac{R_2}{R_1} < 1$ and $m = \frac{M_2}{M_1} > 0$. We will find that this greatly simplifies our analysis. Plugging the mass relationships and non-dimensional constants into our expression for the size distribution, we obtain the following:

$$g(R) = \frac{d^3\delta_1 + m\delta_2}{d^3 + m} \quad (18)$$

Since we have already obtained an expression for the final charge, we need only plug this size distribution into Equation (15) and solve. Consider first the charge on grains of radius R_1, the larger size species. The grain charge expression contains two nested integrals. The integral in the denominator of Equation (15), here represented by I_0, is:

$$I_0(R_j) = \int_0^\infty A_{jk} \left(R_j + R_k\right)^2 g(R_k) dR_k \quad (19)$$

Note that this expression is independent of R_i, the grain species size that we are investigating (which here is R_1). Now consider the remaining integral:

$$I(R_i) = \int_0^\infty \frac{R_j^2 A_{ij} \left(R_i + R_j\right)^2 g(R_j)}{I_0(R_j)} dR_j \quad (20)$$

Finally, we can analytically solve this integral (using the definition of an integral of Dirac delta functions δ_k over a domain containing R_k) and plug this into the expression in Equation (15) for charge on grains of size R_i:

$$Q_{i,final} = e\pi\rho_0 \Bigg(4R_i^2 - \frac{d^3 A_{i1} \left(R_i + R_1\right)^2}{d^3 A_{11} + msA_{12}} - \frac{mA_{i2} \left(R_i + R_2\right)^2}{dsA_{21} + mA_{22}} \Bigg) \quad (21)$$

Before substituting for R_i, we can first expand A_{ij} in terms of the grain sizes R_i and R_j. Recall that this term is symmetric in i and j; that is, $R_{ij} = R_{ji}$. Therefore, we can be certain that $R_{12} = R_{21}$. Furthermore, we can simplify the algebra by defining

$r = r_{12}$ and $s = \frac{1}{4}(1+d)^2 < 1$, which are terms that appear frequently in the reduced expression. The expression reduces significantly in the case where $i = j$:

$$r_{ii} = \frac{2^{1.2} R_i^2}{\left(2R_i^3\right)^{0.4} (2R_i)^{0.8}} = 1, \qquad A_{ii} = R_i^2 \tag{22}$$

$$r = d\left(\frac{2}{s\left(1+d^3\right)}\right)^{0.4}, \qquad A_{12} = rR_1R_2 \tag{23}$$

Finally, we can substitute the grain radii R_1 and R_2 for R_i in Equation (21) to find the net charge on grains of each species:

$$Q_{1,final} = 4e\pi\rho_0 \frac{R_1^2 msr\,(m-d)\,(d-sr)}{\left(d^2+msr\right)(dsr+md)} \tag{24}$$

$$Q_{2,final} = -4e\pi\rho_0 \frac{R_1^2 d^3 sr\,(m-d)\,(d-sr)}{\left(d^2+msr\right)(dsr+md)} \tag{25}$$

V. ANALYSIS

We can demonstrate that these charge equations obey the law of charge conservation; that is, the total charge on grains of size R_1 is equal and opposite to the total charge on grains of size R_2, as we have assumed that all grains start out electrically neutral. The net total charge is $Q_0 = n_1Q_1 + n_2Q_2$, where $n_i = \frac{3M_i}{4\pi\rho_M R_i^3}$ is the number of grains in the mixture with radius R_i. Performing this calculation, we get the following conservation condition:

$$Q_0 = \frac{3M_1}{4\pi\rho_M R_2^3}\left(d^3Q_1 + mQ_2\right) = 0 \tag{26}$$

From Equations (24) and (25), we can see that $d^3Q_1 = -mQ_2$. The cancellation of terms resulting in net charge neutrality supports the validity of the assumptions leading to this model; although real mixtures will have a wide spread in charge within grain sizes, our average charge simplification has clearly not resulted in a violation of charge conservation. In the following sections, we will explore additional differences between our new charge distribution function and the model proposed by Lacks and Levandovsky.

A. Comparison of Continuous and Discrete Models

The original models for granular tribocharging considered only a finite number of discrete grain radii. However, a far more realistic distribution when the mixture is composed primarily of specific sizes is a sum of normal distributions. While even this may not be sufficient to properly model the size distribution found in most naturally-occuring granular mixtures, it is an instructive example in the differences and similarities between our continuous model and the discrete model. We will consider a grain mixture composed of a sum of normal distributions centered around two primary sizes R_1 and R_2, given below:

$$g(R) = k_1 e^{-a_1(R-R_1)^2} + k_2 e^{-a_2(R-R_2)^2} \tag{27}$$

Note that, although it is best practice to normalize this distribution function to $\int_0^\infty g(R)dR = 1$, the fact that the distribution only ever appears in both the numerator and denominator of a ratio suggests that the distribution need only be normalizable, but not actual normalized, as the normalization factor will divide out. We will also specify that $R_2 < R_1$ and define $k = \frac{k_2}{k_1}$ for the sake of convenience and consistency. Here k_i is a factor determining the height of the Gaussian peak corresponding to the distribution of grains of size R_i, so that k is the height of the R_2 peak relative to that of R_1. The coefficients a_1 and a_2 in the exponents are related to the standard deviation of the distributions, a measure of the width of the peaks. Each of these properties can be calculated from the experimentally measured size distribution of a sample of the mixture.

Consider now the case for which $R_1 = 100\mu$m, $R_2 = 50\mu$m, $a_1 = a_2 = 0.005\mu\text{m}^{-2}$, and $k = 8$. The size distribution is shown in Figure 2a for a non-dimensional form of Q_{final}, where:

$$Q^* = \frac{Q_{final}}{4e\pi\rho_0 R_1^2} \tag{28}$$

We can calculate the charge distribution for two cases: the constant contact area assumption made by Lacks and Levandovsky's model, and the size-dependent contact area model using the definition for A_{ij} described above. The final charge distribution is given in Figure 2b. Note that the constant contact area assumption produces a parabolic charge distribution, in which smaller grain sizes acquire an

average negative charge while larger grains become more positively charged. On the other hand, the charge distribution for the size-dependent contact area model appears more closely related to a cubic function, with an additional peak near the small end of the grain size distribution. This means that the smallest grains actually acquire a positive charge, while many large grains are also negatively charged.

B. Polarity Reversal

The apparent reversed charge polarity in the case of size-dependent collision area goes against conventional predictions for granular insulator tribocharging. Lacks and Levandovsky's model predicts that mixture properties have no effect on the polarity, and experiments to date seem to support this assertion [9–12]. In the following sections, we dissect the final charge expression given in Equation (15) to explore the parameters that determine charge polarity. We find that the definition of the area term A_{ij}, as well as the mixture parameters d and m, play a significant role in determining the final charge polarity in a bidisperse (or nearly bidisperse) mixture.

1. *In the Bidisperse Case*

Recall that each of the non-dimensional terms m, d, r, and s is positive for all sizes R_1 and R_2. Therefore, in Equations (24) and (25), while the denominator is necessarily always positive, the negative terms in the numerator make the sign ambiguous at first glance. In previous models, the larger grain size in a bidisperse mixture always acquires a positive charge, a prediction supported by experimental data; however, these models did not include an area term A_{ij}. For our model, we will explore the sign of the numerator of the fraction in Equation (24):

$$sgn(Q_{1,final}) = sgn\left[(m-d)\,(d-sr)\right] \qquad (29)$$

We can expand the expression $d - sr$ in terms of only d as follows:

$$d - sr = d\left(1 - \left[\frac{(1+d)^3}{4\,(1+d^3)}\right]^{0.4}\right) > 0 \qquad (30)$$

It can be trivially shown that the bracketed expression ranges between $1/4$ (as d approaches 0) and

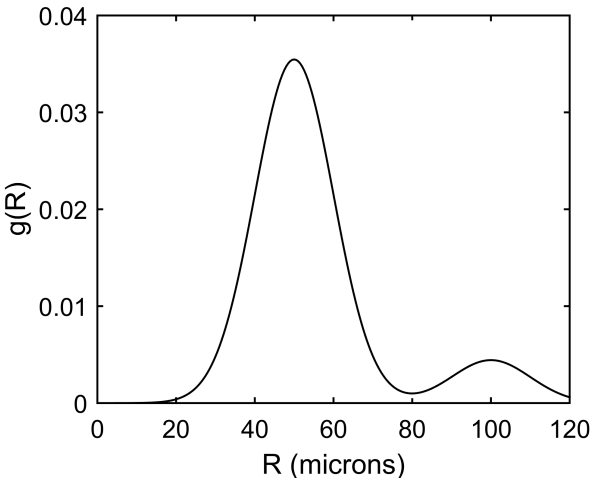

(a)

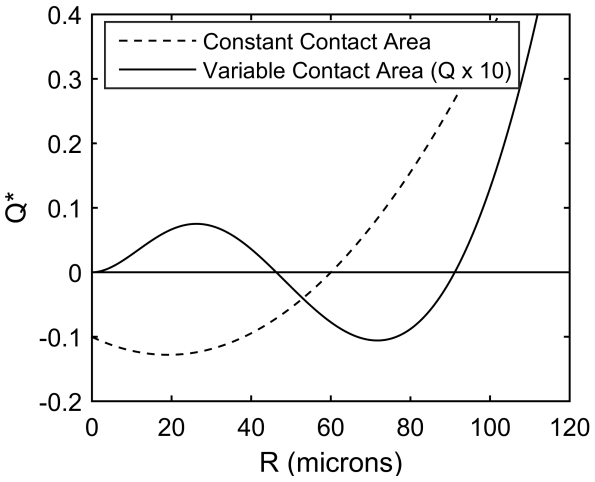

(b)

FIG. 2: Non-dimensional charge distribution $Q^* = Q(R)/4e\pi\rho_0 R_1^2$ for a specified size distribution function. (a) Normalized particle size distribution function $g(R)$ in the form of Equation (27), with $k_2/k_1 = 8$, $a_1 = a_2 = 0.005\mu\text{m}^{-2}$, $R_1 = 100\mu$m, and $R_2 = 50\mu$m. (b) Non-dimensional charge distribution function corresponding to size distribution in (a) (solid line, magnified x10 for clarity). For comparison, the distribution using A_{ij} = constant is overlayed (dashed line). Note the large difference in magnitude, and the additional peak in the distribution for our model at low values of R.

1 (as d approaches 1); we can be sure then that $d-sr$ is positive for all values of d. Therefore, the sign of the charge on grains of size R_1 is entirely determined by the simple expression $m-d$, the difference between the ratio of masses of the two species and the ratio of their radii. Specifically, the larger grains will only achieve the traditionally-predicted positive polarity if the ratio of their mass to the mass of the smaller grains is larger than the ratio of their radius to the radius of the smaller grains. Unfortunately, experiments to date cannot confirm or refute this prediction. This may be due to a general lack of reporting of mass ratios in granular tribocharging experiments, as this value affects only the relative magnitude of average grain charge in the models used and is of significantly less interest than the size ratio d. In the following section, we will find that this polarity reversal also appears in the continuous distribution model, but the exact conditions required to elicit this behavior are more difficult to describe in closed form.

We have already shown (in Section III C 2) that Lacks and Levandovsky's simplification of a single electron transfer per collision is functionally equivalent to the assumption that all contact areas are equivalent. To better understand the influence of the area term on the charge polarity, we can once again calculate the charge on a grain of size R_1, with the area term left as a variable. We are particularly interested in the ratio of contact areas, so let us define an additional non-dimensional term $a_{ij} = \frac{A_{ij}}{A_{11}}$. From Equations (21) and (28):

$$Q_1^* = msa_{12}\left(\frac{ma_{22} - d^3 - sa_{12}(m-d)}{(d^3 + ma_{12}s)(da_{12}s + ma_{22})}\right) \quad (31)$$

Although we have not yet defined A_{ij} in this example, we will make the very basic assumption that, due to the geometry of the grains, collisions between two larger grains cannot (on average) have smaller contact areas than collisions between two smaller grains. Thus we will state only that $a_{22} \leq a_{12} \leq 1$. If the contact areas are equal, then $a_{22} = a_{12} = 1$ and we obtain the expression found by Lacks and Levandovsky:

$$Q_1^* = ms(1-d)\frac{d(1+3d) + m(3+d)}{4(d^3+ms)(ds+m)} > 0 \quad (32)$$

Because $d < 1$ by definition, we see that Equation (32) must always be positive when the contact area term is neglected. When the contact area is not neglected, we can determine what properties A_{ij} must have in order to result in a polarity reversal. Consider now the sign of Equation (31):

$$sgn(Q_1^*) = sgn\left[d\left(s - \frac{d^2}{a_{12}}\right) + m\left(\frac{a_{22}}{a_{12}} - s\right)\right] \quad (33)$$

Now, both $\frac{a_{22}}{a_{12}}$ and s have values less than 1, and $s > d^2$ for all $d < 1$. Therefore, if $a_{12} < 1$ for $d < 1$ and approaches 1 more slowly than $\frac{d^2}{s}$, then the first term will be negative for all values of d greater than some critical value. Furthermore, the second term will be negative above a different critical value for d if a_{22} approaches 1 more slowly than sa_{12}. The relationship between these rates, and the value of m in the mixture, will determine the final value of d for which the entire quantity Q_1 is negative. Because we are dealing with areas here, we expect that a_{22} will have a d^2 dependence and a_{12} will have approximately a d dependence (if any at all). Since a_{12} is approximately of order d^1, we do in fact expect that the first parenthetical expression goes as $s-d$ while the second goes as $d-s$, suggesting that Q_1 is proportional to $m-d$. This reaffirms our observation of the polarity reversal derived above in Equation (29).

2. *In the Continuous Model*

It is important to note that, because we are working with a continuous distribution, the concept of polarity in the sense used in the discrete model is ambiguous. For example, it can be shown that for a size distribution composed of two normal distributions like the one used Figure 2a, the resulting charge distribution always takes on the approximately-cubic form seen in Figure 2b. However, the contribution to the charge from each Gaussian peak varies in a way that reflects the polarity reversal seen in the discrete case. This manifests through a shift in the zeroes of the continuous charge distribution; for example, as the parameters of the size distribution approach the conditions required for a polarity reversal, the negative region of the charge distribution shifts toward the larger grain sizes. This causes larger grains to become more negatively charged, while smaller grains become more positively charged overall. Figure 3 demonstrates the effect of this phenomenon as the size peaks vary in width. This illustrates the importance of using a continuous grain size distribution rather than a

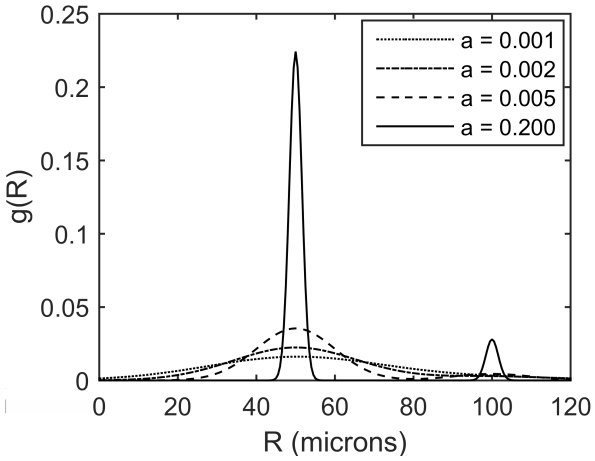

(a)

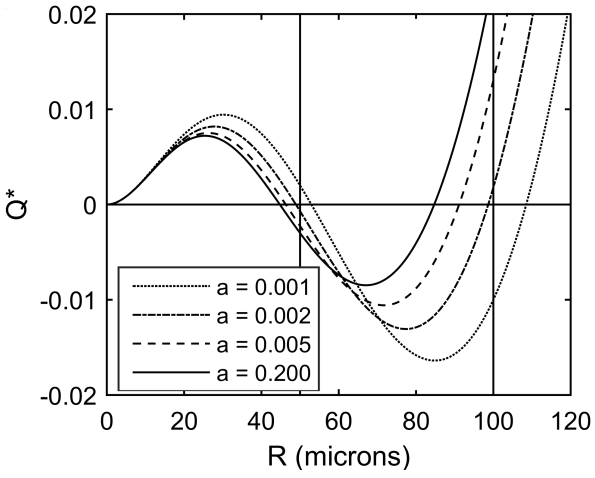

(b)

FIG. 3: Effect of variation in peak width of size distribution on charge polarity, for non-dimensional charge $Q^* = Q(R)/4e\pi\rho_0 R_1^2$. (a) Normalized particle size distribution functions $g(R)$ in the form of Equation (27), with $k_2/k_1 = 8$, $R_1 = 100\mu$m, and $R_2 = 50\mu$m. (b) Non-dimensional charge distribution functions corresponding to the size distributions in (a). Vertical lines at $R = R_1$ and $R = R_2$ provided as reference.

simple discrete size model: the charge distribution is highly dependent on many parameters ignored by the discrete model, especially the width of the peaks in the distribution.

We have also seen how the charge polarity depends primarily on m and d in a primarily two-species distribution when the area term is included. We can plot the non-dimensional charge Q_1^* on grains of radius R_1 against the mixture parameters k and d to better understand their effect. Recal that we can write $m - d$ as $d\left(kd^2 - 1\right)$. Therefore, the polarity reverses (Q_1^* becomes negative) with decreasing k and d. In Figure 4, we see this trend: the critical value of R_2 below which Q_1^* is negative occurs at larger values for decreasing k.

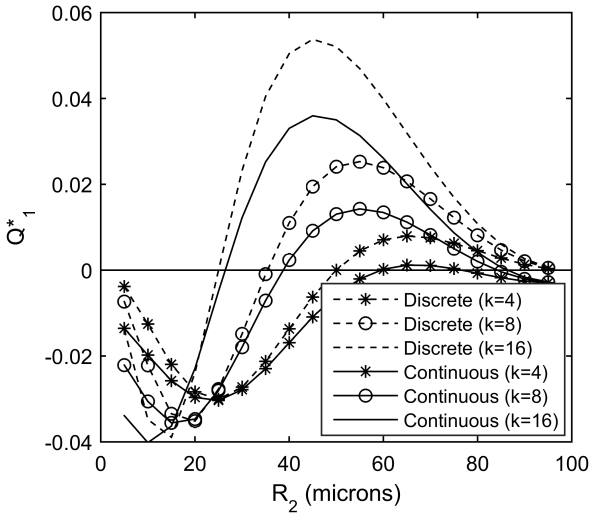

FIG. 4: Non-dimensional net charge $Q_1^* = Q_1(R)/4e\pi\rho_0 R_1^2$ on grains of radius $R_1 = 100\mu$m for a size distribution of the form of Equation (27), with $a = 0.005\mu$m. As the ratio of the peak heights (k) increases, the size ratio ($d = R_2/R_1$) below which large grains charge negatively decreases. Note that the charge predicted by the continuous distribution is very similar to that predicted by the discrete model, with some variation due to the effect of the nonzero peak width (as seen in Figure 3b).

3. Compared to Previous Experiments

The charge transfer model proposed here predicts that, for certain grain size distributions, larger grains charge negatively and smaller grains charge positively. This phenomenon has not been reported in experiments to date, but the lack of existing experimental evidence could be attributed a number of factors. The new polarity distribution is a result of the inclusion of area-dependent charge transfer because, when the area dependence is removed, the predictions made by the continuous distribution

model closely match those of the discrete model. The fact that the polarity reversal in bidisperse mixtures often appears in between size peaks, where the number of grains present is comparatively very small, and that mass ratios are often unreported in experiments, make the polarity reversal difficult to observe. However, experiments on collisions of spheres suggest that the transferred charge is indeed proportional to the contact area [18, 30, 31], suggesting that our implementation of a contact area dependence is accurate. Additionally, small grains may have more irregular surfaces that do not transfer charge as we expect. Many grain charging experiments occur in atmosphere; some experiments have shown that charging in vacuum or a neutral gas produces vastly different charge patterns [15], while others have suggested that humidity from the air adsorbed onto grains creates conductive paths during collisions that may alter the process of charge transfer [8, 24, 33–35]. These possibilities must be explored to determine what conditions are necessary in order to correctly predict grain charging.

In particular, the role of surface water in obfuscating experiment results cannot be understated. Prior experiments indicate that the presence of an electric field in a granular mixture can lead to charge exchange during collisions, leading to a self-reinforcing phenomenon in which the charge separation continues to grow with continued mixing [1, 24]. Zhang, *et al*, proposed a charge transfer mechanism entirely based on the motion of dissociated ions in the surface water layer on the grains, whereby the contact of two grains creates a conductive path across which these ions can move and leave net charge on each grain after separation [24]. This phenomenon may obscure the effect of contact-area-dependent charging processes that would otherwise dominate the charge transfer in dry environments like deserts and dusty airless bodies like the Moon. The fact that charging is known to occur in these dry environments, however, suggests that these models may still be accurate, although care must be taken to eliminate surface water when conducting experiments to compare to the models.

C. Predicted Charge Magnitude as Compared to Experiments

In Figure 2b, we saw that our new contact-area-dependent charge transfer model predicts a much lower charge magnitude than existing models for the same size distribution. In fact, it has been noted that even existing models underestimate the charge magnitude compared to grain charging experiments, leading to speculation regarding the validity of the trapped electron model in general [10]. We believe that the large difference in charge magnitude and the polarity reversal may be related to a single phenomenon ignored by the models. In particular, we suspect that the influence of atmospheric ions or adsorbed humidity encourages charge transfer in a manner that neglects the effect of contact area, as discussed in Section V B 3. This effect has been connected to increased charge separation in a number of experiments [8, 15, 33]. The fact that many experiments have been conducted in atmosphere or in the presence of other gases and have not involved pretreatment of the grains to eliminate adsorbed water suggests that this confounding factor may indeed be present, causing the results to diverge from the idealized case.

VI. CONCLUSION

In the pursuit of a more realistic model for same-material granular insulator tribocharging, we have built upon Lacks and Levandovsky's original model and added size-dependent charge exchange and the ability to consider arbitrary size distributions, rather than discrete, bidisperse mixtures. The predictions made for continuous size distributions are similar to those made for discrete distributions of a similar form. In the limit where the continuous distribution approaches a discrete distribution, the charge predictions converge. We have also modified the underlying model for charge transfer by including a dependence on contact area in determining the number of electrons transferred in each collision. This model predicts that mixtures of two size species with a smaller population of larger grains may display a reversed charge polarity (i.e., large grains charge negatively and small grains charge positively) compared to Lacks and Levandovsky's model. Leading theories on insulator charging suggest that charging in vacuum or under different humidity conditions may lead to different charging behavior, especially charge separation magnitude and polarity of final charge. We are designing an experiment to test the applicability of our model to granular tribocharging under various conditions, particularly in vacuum where the absence of humidity may cause contact area to play a more significant role. Future experiments will include pre-experiment baking of the grains to remove the adsorbed surface water, to ensure charging events are due to grain surface contact only. By experimentally testing for polar-

ity reversal in a humidity-controlled environment, we hope to gain additional evidence in support of, or contradicting, the trapped high-energy model for triboelectric charging in insulators.

VII. ACKNOWLEDGMENTS

We benefitted greatly from discussions with Heinrich Jaeger and Victor Lee regarding experimental investigation of our research. We would also like to acknowledge Daniel Lacks and Artem Levandovsky for their work on granular tribocharging, which was foundational to the development of our model. We would also like to thank Carlos Calle and the NASA Kennedy Space Center for their extensive support of our research. This work was supported by a NASA Space Technology Research Fellowship (NNX15AP69H).

[1] T. Pahtz, H. Herrmann, and T. Shinbrot, Nature Physics **6**, 364 (2010).
[2] J. Kok and N. Renno, Physical Review Letters **100** (2008).
[3] X. Zheng, N. Huang, and Y. Zhou, Journal of Geophysical Research - Atmospheres **108** (2003).
[4] J. Gilbert, S. Lane, R. Sparks, and T. Koyaguchi, Nature **349**, 598 (1991).
[5] S. Liang, J. Zhang, and L. Fan, Industrial & Engineering Chemistry Research **35**, 2748 (1996).
[6] G. Hendrickson, Chemical Engineering Science **61**, 1041 (2006).
[7] D. Saville, M. Al-Adel, and S. Sundaresan, Industrial & Engineering Chemistry Research **41**, 6224 (2002).
[8] P. Cartwright, S. Singh, A. G. Bailey, and L. J. Rose, IEEE Transactions on Industry Applications (1985).
[9] D. J. Lacks and A. Levandovsky, Journal of Electrostatics **65**, 107 (2006).
[10] S. R. Waitukaitis, V. Lee, J. M. Pierson, S. L. Forman, and H. M. Jaeger, Physical Review Letters **112** (2014).
[11] D. J. Lacks, N. Duff, and S. K. Kumar, Physical Review Letters **100** (2008).
[12] K. M. Forward, D. J. Lacks, and R. M. Sankaran, Physical Review Letters **102** (2009).
[13] N. Duff and D. J. Lacks, Journal of Electrostatics **66**, 51 (2008).
[14] J. Kok and D. J. Lacks, Physical Review E **79** (2009).
[15] T. Shinbrot, T. Komatsu, and Q. Zhao, Europhysics Letters **83** (2008).
[16] J. Lowell and W. Truscott, Journal of Physics D: Applied Physics **19**, 1273 (1986).
[17] J. Lowell and W. Truscott, Journal of Physics D: Applied Physics **19**, 1281 (1986).
[18] T. Matsuyama and H. Yamamoto, IEEE Transactions on Industry Applications **30**, 602 (1994).
[19] S. Matsusaka, H. Maruyama, T. Matsuyama, and M. Ghadiri, Chemical Engineering Science **65**, 5781 (2010).
[20] C. F. Gallo and W. L. Lama, IEEE Transactions on Industry Applications (1976).
[21] A. Diaz and R. Felix-Navarro, Journal of Electrostatics **62**, 277 (2004).
[22] J. Henniker, Nature **196** (1962).
[23] T. A. L. Burgo, T. R. D. Ducati, K. R. Francisco, K. J. Clinckspoor, F. Galembeck, and S. E. Galembeck, Langmuir **28**, 7407 (2012).
[24] Y. Zhang, T. Pahtz, Y. Liu, X. Wang, R. Zhang, Y. Shen, R. Ji, and B. Cai, Physical Review X **5** (2015).
[25] H. Zhao, G. S. P. Castle, I. I. Inculet, and A. G. Bailey, IEEE Transactions on Industry Applications **39** (2003).
[26] K. M. Forward, D. J. Lacks, and R. M. Sankaran, Journal of Electrostatics **67**, 178 (2009).
[27] K. M. Forward, D. J. Lacks, and R. M. Sankaran, Journal of Geophysical Research **114** (2009).
[28] K. M. Forward, D. J. Lacks, and R. M. Sankaran, Geophysical Research Letters **36** (2009).
[29] S. R. Waitukaitis and H. M. Jaeger, Review of Scientific Instruments **84** (2013).
[30] H. Watanabe, A. Samimi, Y. L. Ding, M. Ghadiri, and T. Matsuyama, Particle and Particle Systems Characterization , 133 (2006).
[31] S. Matsusaka, M. Ghadiri, and H. Masuda, Journal of Physics D: Applied Physics , 2311 (2000).
[32] D. Gugan, American Journal of Physics **68** (2000).
[33] S. Pence, V. Novotny, and A. Diaz, Langmuir **10**, 592 (1994).
[34] J. A. Wiles, M. Fialkowski, M. R. Radowski, G. M. Whitesides, and B. A. Gryzbowski, Journal of Physical Chemistry B **108**, 20296 (2004).
[35] L. S. McCarty and G. M. Whitesides, Angewandte Chemie International Edition **47**, 2188 (2008).